A DIFFERENTIAL TURBO DETECTION AIDED SPHERE PACKING MODULATED SPACE-TIME CODING SCHEME

*Osamah Alamri, Nan Wu and Lajos Hanzo**

School of ECS, University of Southampton, SO17 1BJ, UK.
Email: lh@ecs.soton.ac.uk
http://www-mobile.ecs.soton.ac.uk

Abstract - A signal construction method that combines orthogonal design with sphere packing has recently shown useful performance improvements over the conventional orthogonal design. In this contribution, we extend this concept and propose a novel Sphere Packing (SP) modulated differential Space-Time Block Coded (DSTBC) scheme, referred to here as (DSTBC-SP), which shows performance advantages over conventional DSTBC schemes. We also demonstrate that the performance of DSTBC-SP systems can be further improved by concatenating sphere packing aided modulation with channel coding and performing SP-symbol-to-bit demapping as well as channel decoding iteratively. We also investigate the convergence behaviour of this concatenated scheme with the aid of Extrinsic Information Transfer (EXIT) Charts. The proposed turbo-detected DSTBC-SP scheme exhibits a 'turbo-cliff' at $E_b/N_0 = 6dB$ and provides E_b/N_0 gains of $23.7dB$ and $1.7dB$ at a BER of 10^{-5} over an equivalent-throughput uncoded DSTBC-SP scheme and a turbo-detected QPSK modulated DSTBC scheme, respectively.

1. INTRODUCTION

During the late 1990s, space-time coding invoking multiple antennas both at the transmitter and the receiver has become a popular technique of attaining transmit diversity [1]. Since then, the pursuit of designing improved space-time modulation schemes has attracted considerable further attention [2]. However, most proposed schemes assumed the availability of perfect channel knowledge at the receiver. In practice the channel impulse response (CIR) recorded for each transmit and receive antenna pair has to be estimated at the receiver using training symbols. However, channel estimation increases both the cost and complexity of the receiver as well as imposing an undesirable transmission overhead and wasting some of the valuable transmit power. As attractive design alternatives, non-coherent schemes that require no CIR knowledge were developed. For example, Tarokh and Jafarkhani [3] proposed differential encoding and decoding for Alamouti's two-transmitter diversity scheme [4], where the transmitted signal can be demodulated both with and without channel state information at the receiver. The non-coherent receiver performs within $3dB$ of the coherent receiver. The scheme advocated in [3] was extended to QAM constellations in [5]. In 2000, Hochwald and Sweldens [6] proposed a differential modulation aided transmit diversity scheme based on unitary space-time codes [7], which can be employed in conjunction with an arbitrary number of transmit antennas. At about the same time, a similar differential scheme was also proposed by Hughes [8] that is based on group codes.

*The financial support of the Ministry of Higher Education of Saudi Arabia as well as that of the EPSRC, UK and the European Union under the auspices of the Newcom and Phoenix projects is gratefully acknowledged.

Iterative decoding of spectrally efficient modulation schemes was considered by several authors. In [9], the employment of the turbo principle was considered for iterative soft demapping in the context of multilevel modulation schemes combined with channel decoding, where a soft demapper was used between the multilevel demodulator and the channel decoder. Recently, studying the convergence behaviour of iterative decoding has attracted considerable attention. In [10], ten Brink proposed the employment of the so-called extrinsic information transfer (EXIT) characteristics between a concatenated decoder's output and input for describing the flow of extrinsic information through the soft-in/soft-out constituent decoders.

The concept of combining orthogonal transmit diversity designs with the principle of sphere packing was introduced by Su *et al.* in [11], where it was demonstrated that the proposed Sphere Packing (SP) aided Space-Time Block Coded (STBC) system, referred to here as (STBC-SP), was capable of outperforming the conventional orthogonal design based STBC schemes of [4, 12]. The authors of [13] proposed a novel system that exploits the advantages of both iterative demapping and decoding [9] as well as those of the STBC-SP scheme of [11]. The STBC-SP demapper of [11] was modified in [13] for the sake of accepting the *a priori* information passed to it from the channel decoder as extrinsic information.

Motivated by the performance improvements reported in [11] and [9], we propose a novel DSTBC scheme that exploits the advantages of both sphere packing modulation as well as those of iterative demapping and decoding. As a benefit of the proposed solution, it will be demonstrated in Section 5 that the proposed turbo detection aided DSTBC-SP scheme is capable of providing E_b/N_0 gains of $23.7dB$ and $1.7dB$ at a Bit Error Rate (BER) of 10^{-5} over an equivalent-throughput uncoded DSTBC-SP scheme and over a turbo-detected conventionally modulated system based on the DSTBC scheme of [3, 5].

This paper is organised as follows. In Section 2, a brief description to orthogonal design using sphere packing modulation is presented, followed by a system overview in Section 3. Section 4 provides our EXIT chart analysis, while our simulation results and discussions are provided in Section 5. Finally, we conclude in Section 6.

2. ORTHOGONAL DESIGN WITH SPHERE PACKING MODULATION

Orthogonal transmit diversity designs can be described recursively [14] as follows. Let $G_1(g_1) = g_1 I_1$, and

$$G_{2^k}(g_1, \ldots, g_{k+1}) = \begin{bmatrix} G_{2^{k-1}}(g_1, \ldots, g_k) & g_{k+1} I_{2^{k-1}} \\ -g_{k+1}^* I_{2^{k-1}} & G_{2^{k-1}}^{\mathcal{H}}(g_1, \ldots, g_k) \end{bmatrix},$$

for $k = 1, 2, 3, \ldots$,where g_{k+1}^* is the complex conjugate of g_{k+1}, $G_{2^{k-1}}^{\mathcal{H}}(g_1, \ldots, g_k)$ is the Hermitian of $G_{2^{k-1}}(g_1, \ldots, g_k)$ and $I_{2^{k-1}}$ is a $(2^{k-1} \times 2^{k-1})$ identity matrix. Then, $G_{2^k}(g_1, g_2, \ldots, g_{k+1})$ constitutes an orthogonal design of size $(2^k \times 2^k)$, which maps the complex variables representing $(g_1, g_2, \ldots, g_{k+1})$ to 2^k transmit antennas. In other words, $g_1, g_2, \ldots, g_{k+1}$ represent $k+1$ complex modulated symbols to be transmitted from 2^k transmit antennas in $T = 2^k$ time slots. It was shown in [11] that the diversity product quantifying coding advantage[1] of an orthogonal transmit diversity scheme is determined by the minimum Euclidean distance of the vectors $(g_1, g_2, \ldots, g_{k+1})$. Therefore, in order to maximise the achievable coding advantage, it was proposed in [11] to use sphere packing schemes that have the best known minimum Euclidean distance in the $2(k+1)$-dimensional real-valued Euclidean space $R^{2(k+1)}$ [15].

In this contribution, differential space-time systems [3, 5] employing two transmit antennas are considered, which are characterised by the generator matrix of [4]

$$G_2(g_1, g_2) = \begin{bmatrix} g_1 & g_2 \\ -g_2^* & g_1^* \end{bmatrix}, \tag{1}$$

and the rows and columns of Equation (1) represent the temporal and spatial dimensions, corresponding to two consecutive time slots and two transmit antennas, respectively. The transmission is initialised by sending arbitrary symbols $g_1(1)$ and $g_2(1)$ using Equation (1) during the 1^{st} and 2^{nd} time slots from the 1^{st} and 2^{nd} transmit antennas. At time $2t+1$, $t = 1, 2, \ldots$, a block of B bits arrives at the encoder, where each $\frac{B}{2}$ bits are independently modulated using a $2^{\frac{B}{2}}$-ary modulation constellation producing $x_1(2t+1)$ and $x_2(2t+1)$. Now, for $t \geq 1$ the transmission symbols $g_1(2t+1)$ and $g_2(2t+1)$ are calculated as follows [5]:

$$\begin{aligned} g_1(2t+1) &= n_f \cdot \left[x_1(2t+1)g_1(2t-1) - x_2(2t+1)g_2^*(2t-1)\right] \\ g_2(2t+1) &= n_f \cdot \left[x_1(2t+1)g_2(2t-1) + x_2(2t+1)g_1^*(2t-1)\right], \end{aligned} \tag{2}$$

where $n_f = 1/\sqrt{|g_1(2t-1)|^2 + |g_2(2t-1)|^2}$. More specifically, $g_1(2t+1)$ and $g_2(2t+1)$ are transmitted from the 1^{st} and 2^{nd} transmit antennas, respectively, at time $2t+1$. By contrast, $-g_2^*(2t+1)$ and $g_1^*(2t+1)$ are transmitted from the 1^{st} and 2^{nd} transmit antennas, respectively, at time $2t+2$.

It was shown in [5] that when the received signals are differentially decoded, the resultant signals will be scaled versions of $x_1(2t+1)$ and $x_2(2t+1)$, which are corrupted by complex Additive White Gaussian Noise (AWGN) similar to the G_2 space-time block code of [4, 12]. This observation implies that the diversity product of DSTBC schemes [3, 5] is determined by the minimum Euclidean distance of all legitimate vectors (x_1, x_2), where the time index is removed for notational simplicity. According to [3, 5] for example, x_1 and x_2 represent independent conventional BPSK modulated symbols and no effort is made to jointly design a symbol constellation for the various combinations of x_1 and x_2. For the sake of generalising our treatment, let us assume that there are L legitimate vectors $(x_{l,1}, x_{l,2})$, $l = 0, 1, \ldots, L-1$, where L represents the number of sphere-packed modulated symbols. The encoder, then, has to choose the modulated symbol associated with each block of B bits from these L legitimate symbols, which determines the signals to be transmitted over the two antennas in two consecutive time slots using Equation (2), where the throughput of the system is given

[1]The diversity product or coding advantage was defined as the estimated gain over an uncoded system having the same diversity order as the coded system [11].

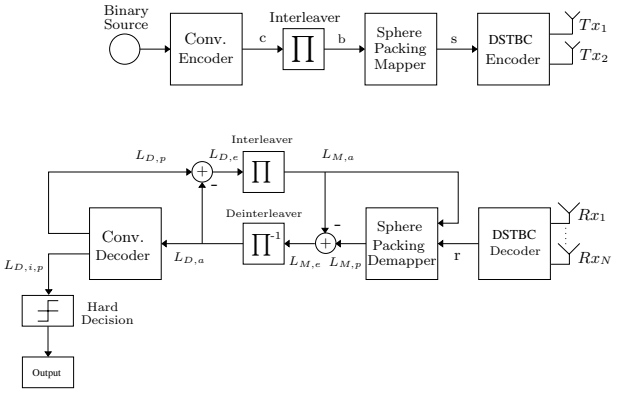

Figure 1: Turbo Detection DSTBC-SP System.

by $(log_2 L)/2$ bits per channel use. In contrast to the independent design of $x_{l,1}$ and $x_{l,2}$ [3, 5], our aim is to design $x_{l,1}$ and $x_{l,2}$ jointly, such that they have the best minimum Euclidean distance from all other $(L-1)$ legitimate symbols, since this minimises the system's error probability. Let $(a_{l,1}, a_{l,2}, a_{l,3}, a_{l,4})$, $l = 0, 1, \ldots, L-1$, be phasor points selected from the four-dimensional real-valued Euclidean space R^4, where each of the four elements $a_{l,1}, a_{l,2}, a_{l,3}, a_{l,4}$ gives one coordinate of the complex-valued phasor points. Hence, $x_{l,1}$ and $x_{l,2}$ may be written as

$$\begin{aligned} \{x_{l,1}, x_{l,2}\} &= T(a_{l,1}, a_{l,2}, a_{l,3}, a_{l,4}) \\ &= \left\{a_{l,1} + ja_{l,2}, a_{l,3} + ja_{l,4}\right\}. \end{aligned} \tag{3}$$

In the four-dimensional real-valued Euclidean space R^4, the lattice D_4 is defined as a sphere packing having the best minimum Euclidean distance from all other $(L-1)$ legitimate constellation points in R^4 [15]. More specifically, D_4 may be defined as a lattice that consists of all legitimate sphere packed constellation points having integer coordinates $[a_1\ a_2\ a_3\ a_4]$ uniquely and unambiguously describing the legitimate combinations of the modulated symbols $x_{l,1}$ and $x_{l,2}$, but subjected to the sphere packing constraint of $a_1 + a_2 + a_3 + a_4 = k$, where k is an even integer. Assuming that $S = \{s^l = [a_{l,1}, a_{l,2}, a_{l,3}, a_{l,4}] \in \mathrm{R}^4 : 0 \leq l \leq L-1\}$ constitutes a set of L legitimate constellation points from the lattice D_4 having a total energy of $E \triangleq \sum_{l=0}^{L-1}(|a_{l,1}|^2 + |a_{l,2}|^2 + |a_{l,3}|^2 + |a_{l,4}|^2)$, and upon introducing the notation

$$C_l = \sqrt{\frac{2L}{E}}(x_{l,1}, x_{l,2}), \qquad l = 0, 1, \ldots, L-1, \tag{4}$$

we have a set of complex constellation symbols, $\{C_l{:}0 \leq l \leq L-1\}$, whose diversity product is determined by the minimum Euclidean distance of the set of L legitimate constellation points in S.

3. SYSTEM OVERVIEW

The schematic of the entire system is shown in Figure 1, where the transmitted source bits are convolutionally encoded and then interleaved by a random bit interleaver. A rate $R = \frac{1}{2}$ recursive systematic convolutional (RSC) code was employed. After channel interleaving, the sphere packing mapper first maps B channel-coded bits $\mathbf{b} = b_{0,\ldots,B-1} \in \{0, 1\}$ to a legitimate constellation point $s^l \in S$ from the lattice D_4, where we have $B = log_2 L$. The mapper then maps the constellation point s^l to complex symbols $x_{l,1}$ and $x_{l,2}$ using Equations (3) and (4). Subsequently, the DSTBC encoder calculates the symbols to be

transmitted according to Equation (2) over $T = 2$ consecutive time slots using two transmit antennas, as shown in Equation (1).

In this treatise, we considered a correlated narrowband Rayleigh fading channel, associated with a normalised Doppler frequency of $f_D = f_d T_s = 0.01$, where f_d is the Doppler frequency and T_s is the symbol duration. The complex fading envelope is assumed to be constant across the transmission period of two sphere packing symbols spanning $T = 4$ time slots. The complex Additive White Gaussian Noise (AWGN) of $n = n_I + jn_Q$ is also added to the received signal, where n_I and n_Q are two independent zero mean Gaussian random variables having a variance of $\sigma_n^2 = \sigma_{n_I}^2 = \sigma_{n_Q}^2 = N_0/2$ per dimension, where $N_0/2$ represents the double-sided noise power spectral density expressed in W/Hz.

As shown in Figure 1, the received complex-valued symbols are first differentially decoded by the DSTBC decoder. Then, the decoded symbols are passed to the sphere packing demapper, where they are demapped to their Log-Likelihood Ratio (LLR) representation for each of the B coded bits per sphere packing symbol. The $a\ priori$ LLR values of the demodulator are subtracted from the $a\ posteriori$ LLR values for the sake of generating the extrinsic LLR values $L_{M,e}$, and then the LLRs $L_{M,e}$ are deinterleaved by a soft-bit deinterleaver, as seen in Figure 1. Next, the soft bits $L_{D,a}$ are passed to the convolutional decoder in order to compute the $a\ posteriori$ LLR values $L_{D,p}$ provided by the Max-Log MAP algorithm [16] for all the channel-coded bits. During the last iteration, only the LLR values $L_{D,i,p}$ of the original uncoded systematic information bits are required, which are passed to a hard decision decoder in order to determine the estimated transmitted source bits. The extrinsic information $L_{D,e}$, is generated by subtracting the $a\ priori$ information from the $a\ posteriori$ information according to $L_{D,p} - L_{D,a}$, which is then fed back to the DSTBC-SP demapper as the $a\ priori$ information $L_{M,a}$ after appropriately reordering them using the interleaver of Figure 1. The sphere packing demapper exploits the $a\ priori$ information for the sake of providing improved $a\ posteriori$ LLR values, which are then passed to the channel decoder and in turn back to the sphere packing demodulator for further iterations. More detailed discussions on the iterative demapping process and how the sphere packing demapper is modified for exploiting the $a\ priori$ knowledge provided by the channel decoder are provided in [13].

4. EXIT CHART ANALYSIS

The main objective of employing EXIT charts proposed by ten Brink [10], is to predict the convergence behaviour of the iterative decoder by examining the evolution of the input/output mutual information exchange between the inner and outer decoders in consecutive iterations. The application of EXIT charts is based on two assumptions, firstly that upon assuming a sufficiently large interleaver length, the $a\ priori$ LLR values become fairly uncorrelated; and secondly that the probability density function (PDF) of the $a\ priori$ LLR values is Gaussian, although in practice these assumptions may not always hold.

The mutual information of $I_{A_M} = I(b; L_{M,a})$, $0 \leq I_{A_M} \leq 1$, between the outer coded and interleaved bits b of Figure 1 and the LLR values $L_{M,a}$ is used to quantify the information content of the $a\ priori$ knowledge at the input of the demapper [17]. By contrast, in order to quantify the information content of the extrinsic LLR values $L_{M,e}$ at the output of the demapper, the mutual information $I_{E_M} = I(b; L_{M,e})$ can be used. Considering I_{E_M} as a function of both I_{A_M} and the E_b/N_0 value encountered, the demapper's extrinsic information transfer characteristic is defined as [10] $I_{E_M} = T_M(I_{A_M}, E_b/N_0)$.

The extrinsic transfer characteristic of the outer channel decoder describes the relationship between the outer channel coded input $L_{D,a}$ and the outer channel decoded extrinsic output $L_{D,e}$. The input of the outer channel decoder is constituted by the $a\ priori$ input $L_{D,a}$ provided by the sphere-packing demapper. Therefore, the extrinsic information transfer characteristic of the outer channel decoder is independent of the E_b/N_0-value and hence may be written as $I_{E_D} = T_D(I_{A_D})$, where $I_{A_D} = I(c; L_{D,a})$, $0 \leq I_{A_D} \leq 1$, is the mutual information between the outer channel coded bits c and the LLR values $L_{D,a}$. Similarly, $I_{E_D} = I(c; L_{D,e})$, $0 \leq I_{E_D} \leq 1$, is the mutual information between the outer channel coded bits c and the LLR values $L_{D,e}$.

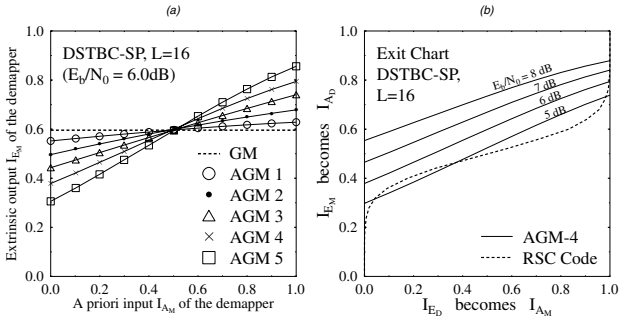

Figure 2: (a) Sphere packing demapper EXIT characteristics for Gray mapping (GM) and different bits to sphere-packing symbol Anti-Gray mapping (AGM)schemes at $E_b/N_0 = 6.0dB$ for $L = 16$. (b) EXIT chart of a turbo-detected RSC channel-coded DSTBC-SP scheme employing Anti-Gray mapping (AGM-4) in combination with the parameters outlined in Table 1.

Figure 2a shows the extrinsic information transfer characteristics of the sphere-packing symbol-to-bit demapper in conjunction with $L = 16$ and different mapping schemes between the interleaver's output and the sphere packing mapper. Observe that Gray mapping does not provide any iteration gain upon increasing the mutual information at the input of the demapper, which was also reported in [9]. The reason for this observation is that the adjacent Gray-coded symbols differ from the one considered in a single bit-position and hence no extrinsic information is gleamed from the remaining identical bits. This situation is reversed, when using different Anti-Gray Mapping (AGM) schemes [9], resulting in different EXIT characteristics, as illustrated by the different slopes seen in Figure 2a. The five different AGM mapping schemes shown in Figure 2a are specifically selected from all the possible mapping schemes for $L = 16$ in order to demonstrate the different extrinsic information transfer characteristics associated with different bit-to-symbol mapping schemes. There are a total of 16! different mapping schemes.

Figure 2b shows the EXIT chart of a turbo-detection aided, channel-coded DSTBC-SP scheme employing the Anti-Gray mapping (AGM-4) of Figure 2a in conjunction with the outer RSC code and the system parameters outlined in Table 1. Ideally, in order for the exchange of extrinsic information between the sphere-packing demapper and the outer RSC decoder to converge at a specific E_b/N_0 value, the extrinsic transfer curve of the sphere-packing demapper recorded at the E_b/N_0 value of interest and the extrinsic transfer characteristic curve of the outer RSC decoder should only intersect at the $(I_{A_D}, I_{E_D}) = (1.0, 1.0)$ point. If this condition is satisfied, then a so-called $convergence\ tunnel$ [10] appears in the EXIT chart. Even if there is no open tunnel in the EXIT chart, but the two EXIT curves intersect at a point infinitesimally close to the $I_{E_D} = 1.0$ line rather than at the $(1.0, 1.0)$ point, then a sufficiently low BER may still be achievable. These types of tunnels are referred to here as $semi\text{-}convergent\ tunnels$. The narrower the

Modulation	Sphere Packing with $L = 16$
No. of Transmitters	2
No. of Receivers	1
Channel	Correlated Rayleigh Fading
Normalised Doppler frequency	0.01
Outer channel code	RSC, $(2, 1, 5)$ $(G_r, G) = (35, 23)_8$
System throughput	1 bit/symbol

Table 1: System parameters

tunnel, the closer the system operates to the Shannon limit and hence a high number of iterations are required for reaching the intersection point. Observe in Figure 2b that a semi-convergent tunnel exists at $E_b/N_0 = 6.0dB$. This implies that according to the predictions of the EXIT chart seen in Figure 2b, the iterative decoding process is expected to converge and hence a low BER may be attained at $E_b/N_0 = 6.0dB$. The validity of this prediction is, however, dependent on how accurately the two EXIT chart assumptions outlined at the beginning of Section 4 are satisfied. These EXIT chart based convergence predictions will be verified by the actual iterative decoding trajectory in Section 5.

5. RESULTS AND DISCUSSION

Without loss of generality, we considered a sphere packing modulation scheme associated with $L = 16$ using two transmit and a single receiver antenna in order to demonstrate the performance improvements achieved by the proposed system. All simulation parameters are listed in Table 1.

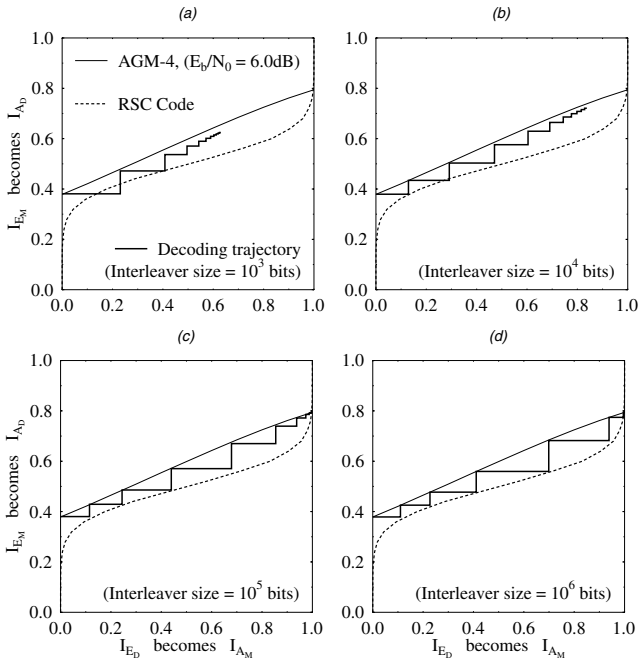

Figure 3: Decoding trajectories of turbo-detected RSC channel-coded DSTBC-SP scheme employing Anti-Gray mapping (AGM-4) in combination with the outer RSC code and the system parameters outlined in Table 1 and operating at $E_b/N_0 = 6.0dB$, when using different interleaver depths.

Since the set of complex constellation symbols, which is constructed from the set of legitimate sphere packing constellation points using Equations (3) and (4) is multiplied by a factor that is inversely proportional to $\sqrt{E}$, namely by $\sqrt{\frac{2L}{E}}$, it is desirable to choose a specific subset of $L = 16$ points from the entire set of legitimate constellation points hosted by D_4, which results in the minimum total energy. It was shown in [15] that there is a total of 24 legitimate symbols[2] hosted by D_4 having an identical minimum energy of $E = 2$. We used a computer search for determining the optimum choice of the $L = 16$ points out of the possible 24 points, which possess the highest minimum Euclidean distance, hence minimising the error probability.

Figure 3 illustrates the actual decoding trajectories of the turbo-detected RSC-coded DSTBC-SP scheme of Figure 2b at $E_b/N_0 = 6.0dB$, when using different interleaver depths. The zigzag-path seen in Figure 3 represents the actual extrinsic information transfer between the sphere-packing demapper and the outer RSC channel decoder. Observe in Figures 3c and 3d that since long interleavers are employed, the assumptions outlined at the beginning of Section 4 are justified and hence the EXIT chart based convergence prediction of the step-wise linear actual decoding trajectory is quite accurate. By contrast, the decoding trajectories shown in Figures 3a and 3b more substantially deviate from the EXIT chart prediction, because shorter interleaver lengths are used. Observe also the difference between Figures 3c and 3d, where more iterations are required for approaching the intersection point, when the interleaver depth drops from 10^6 bits to 10^5 bits. The influence of interleaver depth on system's attainable performance is further highlighted in Figure 4. More specifically, Figure 4 illustrates the achievable BER of the turbo-detected RSC channel-coded DSTBC-SP scheme of Figure 3, when operating at $E_b/N_0 = 6.0dB$ and using different interleaver depths as well as different number of iterations. According to Figure 4, $four$ more iterations are necessitated by the system employing an interleaver depth of 10^5 bits in order to achieve a BER comparable to that of the system employing an interleaver depth of 10^6 bits, when operating at $E_b/N_0 = 6.0dB$.

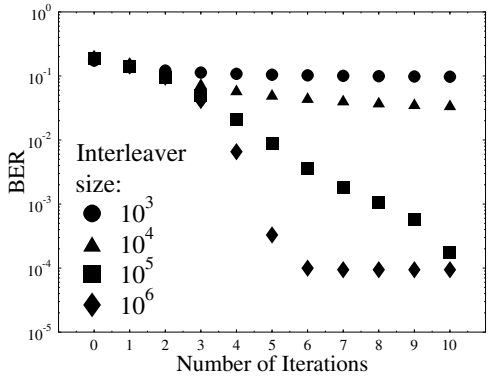

Figure 4: Achievable BER of turbo-detected RSC channel-coded DSTBC-SP scheme employing Anti-Gray mapping (AGM-4) in combination with the outer RSC code and the system parameters outlined in Table 1 and operating at $E_b/N_0 = 6.0dB$ with different interleaver depths and number of iterations.

Figure 5 compares the attainable performance of the proposed RSC-coded DSTBC-SP scheme employing both Anti-Gray Mapping (AGM-4) and Gray Mapping (GM) against that of an iden-

[2]In simple terms, the sphere centred at $(0, 0, 0, 0)$ has 24 spheres around it, centred at the points $(+/-1, +/-1, 0, 0)$, where any choice of signs and any ordering of the coordinates is legitimate [7, p.9].

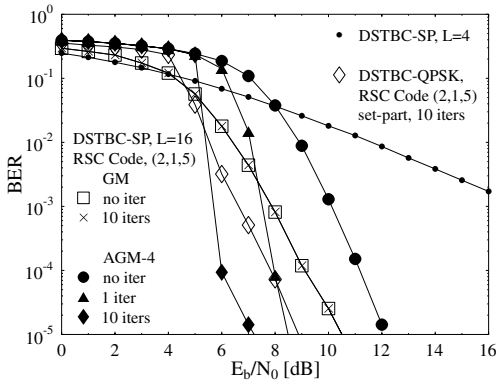

Figure 5: Performance comparison of Anti-Gray Mapping (AGM-4) and Gray Mapping (GM) based RSC-coded DSTBC-SP schemes in conjunction with $L = 16$ against an identical-throughput 1 bit/symbol (BPS) uncoded DSTBC-SP scheme using $L = 4$ and against RSC-coded QPSK modulated DSTBC scheme, when employing the system parameters outlined in Table 1 and using an interleaver depth of $D = 10^6$ bits.

tical-throughput 1 Bit Per Symbol (1BPS) uncoded DSTBC-SP scheme using $L = 4$ and against an RSC-coded QPSK modulated DSTBC scheme, when employing the system parameters outlined in Table 1 and using an interleaver depth of $D = 10^6$ bits. The QPSK modulated DSTBC system employs a set-partitioning mapping scheme reminiscent of Trellis Coded Modulation (TCM) [18]. Observe in Figure 5 by comparing the two Gray Mapping (GM) DSTBC-SP curves that no BER improvement was obtained, when 10 turbo-detection iterations were employed in conjunction with Gray Mapping. This phenomenon was also reported in [9] and it becomes evident from the horizontal curve characterising Gray mapping in Figure 2a. By contrast, Anti-Gray Mapping (AGM-4) of Figure 2a achieved a useful performance improvement in conjunction with iterative demapping and decoding. Explicitly, Figure 5 demonstrates that a coding advantage of about $23.7dB$ was achieved at a BER of 10^{-5} after 10 iterations by the RSC-coded AGM-4 DSTBC-SP system over the uncoded DSTBC-SP for transmission over the correlated Rayleigh fading channel considered. Additionally, a coding advantage of approximately $3.3dB$ and $1.7dB$ were attained over the 1BPS-throughput RSC-coded GM DSTBC-SP scheme and the RSC-coded QPSK modulated DSTBC scheme, respectively.

6. CONCLUSION

In this paper we proposed a novel system that exploits the advantages of both iterative demapping and turbo detection [9], as well as those of the sphere packing modulation proposed in [11]. Our investigations demonstrated that significant performance improvements may be achieved, when the AGM DSTBC-SP scheme is combined with outer channel decoding and iterative demapping, as compared to the Gray-Mapping based systems. Subsequently, EXIT charts were used to search for the optimum bit-to-symbol mapping schemes that converge at the lowest possible E_b/N_0 values. Several DSTBC-SP mapping schemes covering a wide range of extrinsic transfer characteristics were investigated. When using an appropriate bit-to-symbol mapping scheme and 10 turbo detection iterations, E_b/N_0 gains of about $23.7dB$ and $1.7dB$ were obtained by the RSC-coded DSTBC-SP scheme over the identical-throughput 1 bit/symbol uncoded DSTBC-SP benchmarker scheme and over a turbo-detected system based on the DSTBC scheme of [3, 5]. Our future research includes the employment of novel precoding techniques between the outer channel code and the sphere packing mapper for the sake of improving the system's performance while, maximising its throughput and minimising its delay.

7. REFERENCES

[1] L. Hanzo, T. H. Liew, and B. L. Yeap, *Turbo Coding, Turbo Equalisation and Space-Time Coding: for Transmission over Fading Channels*. Chichester, England: John Wiley and Sons Ltd and IEEE Press, NY, USA, 2002.

[2] B. M. Hochwald, G. Gaire, B. Hassibi, and E. T. L. Marzetta, "Special issue on space-time transmission, reception, coding and signal processing," *IEEE Transactions on Information Theory*, vol. 49, pp. 2329–2806, Oct 2003.

[3] V. Tarokh and H. Jafarkhani, "A differential detection scheme for transmit diversity," in *IEEE Journal on Selected Areas in Communications*, vol. 18, pp. 1169–1174, July 2000.

[4] S. Alamouti, "A simple transmit diversity technique for wireless communications," *IEEE Journal on Selected Areas in Communications*, vol. 16, no. 8, pp. 1451–1458, 1998.

[5] C.-S. Hwang, S. H. Nam, J. Chung, and V. Tarokh, "Differential space time block codes using nonconstant modulus constellations," in *IEEE Transactions on Signal Processing*, vol. 51, pp. 2955–2964, Nov 2003.

[6] B. Hochwald and W. Sweldens, "Differential unitary space-time modulation," *IEEE Transactions on Communications*, vol. 48, pp. 2041–2052, Dec 2000.

[7] B. Hochwald and T. Marzetta, "Unitary space-time modulation for multiple-antenna communications in Rayleigh flat fading," *IEEE Transactions on Information Theory*, vol. 46, pp. 543–564, Mar 2000.

[8] B. Hughes, "Differential space-time modulation," *IEEE Transactions on Information Theory*, vol. 46, pp. 2567–2578, Nov 2000.

[9] S. ten Brink, J. Speidel, and R.-H. Yan, "Iterative demappping and decoding for multilevel modulation," in *IEEE Global Telecommunications Conference*, vol. 1, (Sydney, Australia), pp. 579–584, 8-12 Nov 1998.

[10] S. ten Brink, "Designing iterative decoding schemes with the extrinsic information transfer chart," *AEÜ International Journal of Electronics and Communications*, vol. 54, pp. 389–398, Nov 2000.

[11] W. Su, Z. Safar, and K. J. R. Liu, "Space-time signal design for time-correlated Rayleigh fading channels," in *IEEE International Conference on Communications*, vol. 5, (Anchorage, Alaska), pp. 3175–3179, 2003.

[12] V. Tarokh, H. Jafarkhani, and A. Calderbank, "Space-time block codes from orthogonal designs," *IEEE Transactions on Information Theory*, vol. 45, pp. 1456–1467, Jul 1999.

[13] O. Alamri, B. L. Yeap, and L. Hanzo, "Turbo detection of channel-coded space-time signals using sphere packing modulation," in *IEEE Vehicular Technology Conference*, vol. 4, (Los Angeles, USA), pp. 2498–2502, Sep 2004.

[14] W. Su and X. G. Xia, "On space-time block codes from complex orthogonal designs," *Wireless Personal Communications, (Kluwer Academic Publishers)*, vol. 25, pp. 1–26, April 2003.

[15] J. H. Conway and N. J. Sloane, *Sphere Packings, Lattices and Groups*. Springer-Verlag, 1999.

[16] P. Robertson, E. Villebrun, and P. Hoeher, "A comparison of optimal and sub-optimal MAP decoding algorithms operating in the log domain," in *Proceedings of International Conference on Communications*, (Seattle, USA), pp. 1009–1013, Jun 1995.

[17] T. M. Cover and J. A. Thomas, *Elements of information theory*. New York: Wiley, 1991.

[18] G. Ungerboeck, "Channel coding with multilevel/phase signals," in *IEEE Transactions on Information Theory*, vol. 28, pp. 55–67, Jan 1982.